INTERNATIONAL JOURNAL FOR NUMERICAL METHODS IN FLUIDS
Int. J. Numer. Meth. Fluids 2010; **63**:313–340
Published online 5 June 2009 in Wiley InterScience (www.interscience.wiley.com). DOI: 10.1002/fld.2071

Simple and efficient solution of the shallow water equations with source terms

Sang-Heon Lee[1] and Nigel G. Wright[2,*,†]

[1]*University of Nottingham, Nottingham, U.K.*
[2]*UNESCO-IHE, Institute for Water Education, Delft, The Netherlands*

SUMMARY

A simple and efficient method to solve the one-dimensional shallow water equations with source terms is presented. To avoid a fractional step method for the discretization of the source terms, a homogeneous form of the shallow water equations is proposed and well-known conservative numerical schemes are modified to solve the new form of the equations. The modification to the homogeneous form equations combines the source terms with the flux term and solves them by the same solution structure of the numerical scheme. As a result, the source terms are automatically discretized to achieve perfect balance with flux terms without any special treatment and the method does not introduce numerical errors. The proposed method is verified against several benchmark tests and shows good agreement with analytical solutions. Copyright © 2009 John Wiley & Sons, Ltd.

Received 4 April 2008; Revised 6 March 2009; Accepted 10 March 2009

KEY WORDS: shallow water equations; source terms; Roe's solver; HLL solver; Lax–Wendroff scheme; MacCormack scheme; Godunov

1. INTRODUCTION

Finite volume schemes have been widely used for modelling of shallow water flows because of their conservative properties. Especially, Godunov-type schemes based on approximate Riemann solvers [1, 2], which have been developed in the field of aeronautics have been able to deal with transcritical and highly unsteady flows. However, the inclusion of the source terms causes difficulties in finding solutions because it makes the governing equations an inhomogeneous system. In particular, the source terms relevant to the channel geometry cause numerical errors in steady flow problems, when an exact balance of the flux gradient and the source terms is not achieved.

*Correspondence to: Nigel G. Wright, UNESCO-IHE, Delft, The Netherlands.
†E-mail: n.wright@unesco-ihe.org

Contract/grant sponsor: Korean Government

The treatment of geometric source terms has been studied by many researchers. Nujic [3] noted the difficulties in treating variable bottom geometry and suggested that the $0.5gh^2$ term in the flux function should be removed and combined with the source terms. LeVeque [4] inserted an additional discontinuity at the centre of each cell to incorporate source terms into the wave propagation algorithm and avoid the need for fractional steps. LeVeque's method is complicated to implement and shows less robustness when used for steady transcritical flows containing shocks. The upwind approach for source term discretization has been widely used since Bermudez and Vazquez [5] showed that the upwind treatment of source terms produces better results than the pointwise method in a rectangular channel with bed slope variation. Then, Garcia-Navarro and Vazquez-Cendon [6], Hubbard and Garcia-Navarro [7] extended the upwind approach to non-prismatic channels and high-resolution schemes. Burguete and Garcia-Navarro [8, 9] proposed a decomposition technique for the I_2 term and applied the upwind method to arbitrary channel geometry. The upwinding of source terms shows very robust and accurate solutions. However, this method is complex because the source terms must be calculated separately according to the characteristic properties and it is necessary to correct the formulation when using a higher-order scheme. Meanwhile, Zhou *et al.* [10] suggested the surface gradient method for linear reconstruction of data in MUSCL-type schemes and Capart *et al.* [11] reconstructed the geometric source terms by considering the balance of hydrostatic pressure with the approximated water surface level.

In this paper, a different technique for solving the source term problem is presented. The shallow water equations including the source terms are modified to an homogeneous form and solved using well-known numerical schemes. Gascon and Coberan [12] developed an analogous scheme for a nozzle flow problem. They proposed a new flux formed by adding the primitive of the source terms to the flux terms, which was used to modify the governing equations for a compressible gas. An alternative method is developed here for the shallow water equations. This differs from Gascon and Coberan [12] in that the modification is performed by changing the source terms into a differential form similar to the flux term, which leads to a simpler and more efficient form of numerical scheme. Moreover, to secure exact numerical balance, new expressions for the source flux terms and corresponding channel geometry are presented. Consequently, the source terms are treated as a flux term and combined with the original numerical flux to form an integrated numerical flux representing real flow conditions. The integrated intercell numerical flux function including source term effects is obtained by modifying the well-known conservative numerical schemes. In Section 2, the original form of the shallow water equations is presented, while this is modified into an homogeneous form in Section 3. Section 4 presents several conservative schemes to solve the homogeneous form equations. In Section 5, the modified forms of these schemes are applied to benchmark tests to verify their accuracy and ability.

2. THE ONE-DIMENSIONAL SHALLOW WATER EQUATIONS

The one-dimensional shallow water equations that describe the flow in an open channel can be written in the following vector form as:

$$\frac{\partial \mathbf{U}}{\partial t} + \frac{\partial \mathbf{F}}{\partial x} = \mathbf{S} \tag{1}$$

DOI: 10.1002/fld

with

$$\mathbf{U}=\begin{pmatrix}A\\Q\end{pmatrix},\quad \mathbf{F}=\begin{pmatrix}Q\\Q^2/A+gI_1\end{pmatrix}\quad\text{and}\quad \mathbf{S}=\begin{pmatrix}0\\gA(S_o-S_f)+gI_2\end{pmatrix}$$

where A is the wetted cross-sectional area, Q is the discharge, S_o is the bed slope and S_f is the friction slope. The hydrostatic pressure terms I_1 and I_2 are defined as

$$I_1=\int_0^h (h-\eta)\sigma\,\mathrm{d}\eta\quad\text{and}\quad I_2=\int_0^h (h-\eta)\frac{\partial\sigma}{\partial x}\mathrm{d}\eta$$

where h is the water depth and $\sigma=\sigma(x,\eta)$ is the channel width at distance η above the channel bottom.

The shallow water equations (1) form an inhomogeneous hyperbolic equation system due to the existence of the source terms **S**. The inclusion of the source terms makes it difficult to find the correct solutions to open channel flow over irregular geometry. The causes of the difficulties can be summarized in the following two categories: complicated definition of the geometric source terms and incompatibility with the numerical methods based on homogeneous equations. First, the hydraulic pressure terms, I_1 and I_2, have complicated forms, especially the I_2 term that includes the integral of a derivative, which is very difficult to evaluate for non-rectangular channels. Consequently, the most efficient way to calculate geometric source terms is to replace the I_2 term by other terms having simpler definition. Second, most numerical methods are developed on the basis of homogeneous governing equations without source terms. As a result, the numerical techniques cannot solve the inhomogeneous equations with source terms such as the shallow water equations directly. This problem leads to a fractional step method that consists of two steps: calculation of the homogeneous part with the numerical methods based on homogeneous governing equations and subsequent addition of the source term effects. However, it is very difficult to achieve the balance of numerical flux and source terms, especially when the source terms are treated by a pointwise approach. This is because numerical balance is achieved when the following two conditions are satisfied: first, the update of the source terms should be performed with the same data used for the calculation of numerical flux and second, the discretization of the source terms should be performed in the same way as for the flux term. The simplest way to avoid this difficulty is to modify the source terms into the form of a flux, i.e. differential form, and combine it with flux term **F**. This modification leads to the homogeneous form of the shallow water equations. In the next section, the shallow water equations are modified to homogeneous form and a new definition for source the flux term will be presented.

3. HOMOGENEOUS FORM OF THE SHALLOW WATER EQUATIONS

The shallow water equations (1) can be modified to the following homogeneous form

$$\frac{\partial\mathbf{U}}{\partial t}+\frac{\partial\mathbf{H}}{\partial x}=0\quad\text{with }\mathbf{H}=(\mathbf{F}-\mathbf{R}) \tag{2}$$

where $\mathbf{R}=(0,R)^{\mathrm{T}}$ represents the flux vector related to the source terms, which can drive or impede the flow of water. By modification to the homogeneous form, the source terms can be regarded as a flux and solved by the same solution structure used for the flux vector **F**.

DOI: 10.1002/fld

The modified shallow water equations (3) can be numerically discretized conservatively by using a finite volume method

$$\mathbf{U}_i^{n+1} = \mathbf{U}_i^n - \frac{\Delta t}{\Delta x}(\mathbf{H}_{i+1/2}^* - \mathbf{H}_{i-1/2}^*) \tag{3}$$

with $\mathbf{H}_{i+1/2}^* = \mathbf{F}_{i+1/2}^* - \mathbf{R}_{i+1/2}^*$, where $\mathbf{F}^*$ and $\mathbf{R}^*$ are the intercell numerical flux corresponding to flux terms $\mathbf{F}$ and $\mathbf{R}$, respectively. The integrated numerical flux $\mathbf{H}^*$ represents the net flow of mass and momentum through the cell interface including the effect of the source terms. The integrated numerical flux $\mathbf{H}^*$ can be obtained by modifying the numerical flux functions developed for homogeneous governing equations because the equation system (2) and (3) have similar form to the homogeneous conservation law

$$\frac{\partial \mathbf{U}}{\partial t} + \frac{\partial \mathbf{F}}{\partial x} = 0$$

and its discretized form

$$\mathbf{U}_i^{n+1} = \mathbf{U}_i^n - \frac{\Delta t}{\Delta x}(\mathbf{F}_{i+1/2}^* - \mathbf{F}_{i-1/2}^*) \tag{4}$$

3.1. Definition of source flux vector R

While formulating the equations in homogenous form is relatively straightforward, establishing the components of **R** correctly requires more careful consideration. In fact, it is the latter that is the crucial aspect of the method proposed here. To obtain the correct expression of R, which is a component of the source flux vector **R**, first of all, the channel geometry should be reconstructed to be compatible with the homogeneous form equations. The transformation of the equations into homogeneous form effectively removes the external forces on the control volume and instead represents these through the flux term: this implies that there is no additional source of mass or momentum inside a control volume (or, cell) and only the flux terms can contribute to the update of the conserved variables, **U**. To satisfy this condition, a piecewise constant channel geometry as shown in Figure 1 is considered. In the figure, all the factors of the channel geometry, i.e. bed level, width, shape, etc., have constant values in a cell and the interface between two neighbouring cells is considered as a discontinuity because any variation of the channel geometry in a cell causes the addition of momentum, which is contradictory to the assumption of the homogeneous form equations.

The flux term R can be defined based on the piecewise constant channel geometry by using the following two steps: defining ΔR at cell interface and decomposing it properly into two nodal forces. First, the definition of force ΔR can be obtained by comparing Equation (1) and (3):

$$\frac{\partial R}{\partial x} = gA(S_o - S_f) + gI_2 \tag{5}$$

To avoid complicated calculation of the I_2 term, it should be modified by using the Leibnitz theorem for differentiation of an integral [13]:

$$I_2 = \frac{\partial I_1}{\partial x} - A\frac{\partial h}{\partial x}$$

DOI: 10.1002/fld

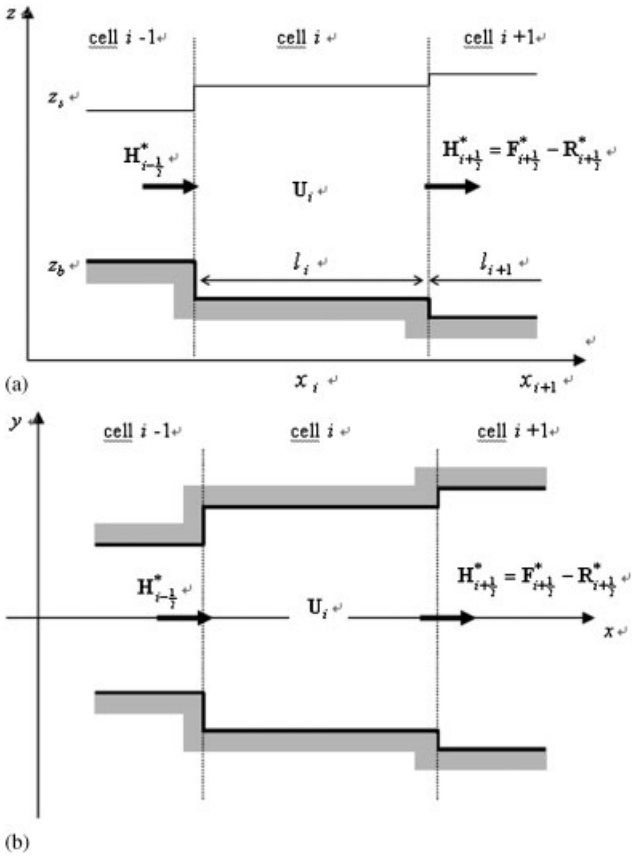

Figure 1. Reconstruction of geometry: (a) section view and (b) plan view.

Consequently, Equation (5) can be rewritten as

$$\frac{\partial R}{\partial x} = g\left(\frac{\partial I_1}{\partial x} - A\frac{\partial z_s}{\partial x} - AS_f\right) \tag{6}$$

where $\partial z_s/\partial x$ is the slope of free surface elevation $z_s = z_b + h$. ΔR at cell interface $i+\frac{1}{2}$ can be obtained by integrating Equation (6):

$$\int_{x_i}^{x_{i+1}} \left(\frac{\partial R}{\partial x}\right) \mathrm{d}x = \int_{x_i}^{x_{i+1}} g\left(\frac{\partial I_1}{\partial x} - A\frac{\partial z_s}{\partial x} - AS_f\right) \mathrm{d}x$$

The integration is performed over the piecewise constant geometry between two nodes x_i and x_{i+1}, and $\Delta R_{i+1/2}$ can be approximated as

$$\Delta R_{i+1/2} = R_{i+1} - R_i = g(\Delta I_1 - \Omega_o - \Omega_f)_{i+1/2}$$

DOI: 10.1002/fld

with

$$\Omega_{oi+1/2}=0.5(A_i+A_{i+1})\Delta z_{s_{i+1/2}}$$

$$\Omega_{fi+1/2}=0.5\Delta x(A_i S_{fi}+A_{i+1}S_{fi+1})$$

where $g\Omega_o$ and $g\Omega_f$ represent the momentum flux due to the water level difference and friction force between two cell centres x_i and x_{i+1}, respectively. The above equations are based on the assumption of a uniform mesh, but it is possible to extend the method to non-uniform meshes by integrating Equation (6) over the relevant cells. This is not the main focus of this paper; hence, it is not presented, but this does not lead to a loss of generality. Similarly, $\Delta R_{i-1/2}$ at cell interface between two cells $i-1$ and i can be expressed as

$$\Delta R_{i-1/2}=R_i-R_{i-1}=g(\Delta I_1-\Omega_o-\Omega_f)_{i-1/2}$$

The next step is to decompose $\Delta R_{i+1/2}$ and $\Delta R_{i-1/2}$ terms into the three ideal forces R_{i-1}, R_i and R_{i+1}, which are essential to update the conserved variable $\mathbf{U}_i$. The decomposition can be performed by considering the numerical balance of $\mathbf{F}$ and $\mathbf{R}$ terms and the direction of Ω_o and Ω_f terms:

$$R_{i-1}=gI_{1i-1}-g(\Omega_o+\Omega_f)_{i-1/2}$$

$$R_i=gI_{1i}$$

$$R_{i+1}=gI_{1i+1}+g(\Omega_o+\Omega_f)_{i+1/2}$$

The $g(\Omega_o+\Omega_f)$ term representing the momentum flux due to the water level difference and friction force is not included in R_i term because it should be considered as a pressure force exerted by the neighbouring cells R_{i+1} and R_{i-1}. As a result, the momentum flux R does not have an absolute value but a relative value. For example, to update the variable $\mathbf{U}_{i+1}$, the values of the three ideal forces R_i, R_{i+1} and R_{i+2} are needed and these can be calculated by decomposing two terms $\Delta R_{i+1/2}$ and $\Delta R_{i+3/2}$ and the value of the term R_i will be changed to $R_i=gI_{1i}+g(\Omega_o+\Omega_f)_{i+1/2}$. Similarly, to update the variable $\mathbf{U}_{i-1}$, the three terms $\mathbf{U}_{i-2}$, $\mathbf{U}_{i-1}$ and $\mathbf{U}_i$ are needed and the value of the term R_i will be changed to $R_i=gI_{1i}-g(\Omega_o+\Omega_f)_{i-1/2}$.

4. CONSERVATIVE SCHEMES

In the previous section, a homogeneous form of the shallow water equations and the definition of the source flux have been presented. This section is devoted to the solution of the homogeneous form equations and it can be performed through simple modification of the well-known numerical schemes developed on the basis of the shallow water equations without source terms. The modification can be performed by replacing the flux term $\mathbf{F}$ and the variable difference $\Delta\mathbf{U}$ with the integrated flux $\mathbf{H}$ and the modified difference $\Delta\mathbf{U}'$. $\Delta\mathbf{U}'$ represents the net difference of the conserved variables $\Delta\mathbf{U}$ including the effect of the channel geometry and can be obtained from the relation between $\Delta\mathbf{H}$ and $\Delta\mathbf{F}$. To verify the applicability of the proposed method to various numerical schemes, approximate Riemann solver-based schemes (Roe and HLL) and TVD

DOI: 10.1002/fld

second-order schemes (Lax–Wendroff and MacCormack) are presented. In order to demonstrate the modification process, the original numerical scheme is introduced first and, then, changed to the homogeneous form.

4.1. Roe's approximate Riemann solver

4.1.1. Original Roe's scheme. Roe [2] constructed an approximate Jacobian $\tilde{\mathbf{J}}$ which satisfies the relation $\Delta\mathbf{F}=\tilde{\mathbf{J}}\Delta\mathbf{U}$ and is diagonalizable with real eigenvalues. The main idea of Roe's method is to split the flux difference at each cell interface by using the approximate Jacobian matrix and which can be expressed as

$$\Delta\mathbf{F}=\tilde{\mathbf{J}}\Delta\mathbf{U}=\tilde{\mathbf{J}}^{+}\Delta\mathbf{U}+\tilde{\mathbf{J}}^{-}\Delta\mathbf{U}$$

where $\tilde{\mathbf{J}}^{\pm}$ represents the positive or negative portion of the Jacobian matrix. $\tilde{\mathbf{J}}^{\pm}$ can be obtained by using the diagonal matrix of the eigenvalues

$$\tilde{\mathbf{J}}^{\pm}=\mathbf{R}\boldsymbol{\Lambda}^{\pm}\mathbf{R}^{-1}$$

where $\mathbf{R}$ is the matrix of right eigenvectors and $\boldsymbol{\Lambda}^{\pm}$ represents the matrix having only the positive or negative eigenvalues on the diagonal. $\mathbf{R}$ and $\boldsymbol{\Lambda}^{\pm}$ satisfy the following relations:

$$\tilde{\mathbf{J}}=\tilde{\mathbf{J}}^{+}+\tilde{\mathbf{J}}^{-}=\mathbf{R}(\boldsymbol{\Lambda}^{+}+\boldsymbol{\Lambda}^{-})\mathbf{R}^{-1}$$

By using these relations, the numerical flux at the cell interface $i+\frac{1}{2}$ between two cells i and $i+1$, $\mathbf{F}^{*}_{i+1/2}$, can be written as

$$\mathbf{F}^{*}_{i+1/2}=\mathbf{F}_{i}+\tilde{\mathbf{J}}^{-}_{i+1/2}(\mathbf{U}_{i+1}-\mathbf{U}_{i}) \tag{7}$$

$$\mathbf{F}^{*}_{i+1/2}=\mathbf{F}_{i+1}-\tilde{\mathbf{J}}^{+}_{i+1/2}(\mathbf{U}_{i+1}-\mathbf{U}_{i}) \tag{8}$$

or by averaging (7) and (8)

$$\mathbf{F}^{*}_{i+1/2}=\tfrac{1}{2}(\mathbf{F}_{i+1}+\mathbf{F}_{i})-\tfrac{1}{2}|\tilde{\mathbf{J}}_{i+1/2}|\Delta\mathbf{U}_{i+1/2} \tag{9}$$

By projecting onto the right eigenvectors, the variable differences $\Delta\mathbf{U}$ can be rewritten as

$$\Delta\mathbf{U}_{i+1/2}=\mathbf{U}_{i+1}-\mathbf{U}_{i}=\sum_{k}(\tilde{\alpha}_{k}\tilde{e}_{k})_{i+1/2} \tag{10}$$

and the numerical flux function (9) can be rewritten as the following characteristic form as:

$$\mathbf{F}^{*}_{i+1/2}=\frac{1}{2}(\mathbf{F}_{i+1}+\mathbf{F}_{i})-\frac{1}{2}\sum_{k}(\tilde{\alpha}_{k}|\tilde{\lambda}_{k}|\tilde{e}_{k})_{i+1/2}$$

The approximate Jacobian matrix has eigenvalues and eigenvectors of the form

$$\tilde{\lambda}_{1,2}=\tilde{u}\pm\tilde{c}$$

$$\tilde{e}_{1,2}=(1,\tilde{\lambda}_{1,2})^{\mathrm{T}}$$

DOI: 10.1002/fld

where the average values $\tilde{u}$ and $\tilde{c}$ can be obtained from the condition $\Delta\mathbf{F}=\tilde{\mathbf{J}}\Delta\mathbf{U}$:

$$\tilde{u}_{i+1/2}=\frac{Q_{i+1}/\sqrt{A_{i+1}}+Q_i/\sqrt{A_i}}{\sqrt{A_{i+1}}+\sqrt{A_i}}$$
$$\tilde{c}^2_{i+1/2}=\begin{cases} g\dfrac{I_{i+1}-I_i}{A_{i+1}-A_i} & \text{if } A_{i+1}-A_i\neq 0 \\ c_i^2=c_{i+1}^2 & \text{if } A_{i+1}-A_i=0 \end{cases} \tag{11}$$

Note that Equation (11) can be used only for a prismatic channel case because, in case of a non-prismatic channel, $(I_{i+1}-I_i)/(A_{i+1}-A_i)$ and $\tilde{c}^2_{i+1/2}$ can have negative value. Alternatively, several expressions for $\tilde{c}$ are found in available literature and the one presented by Garcia-Navarro and Vazquez-Cendon [6] is used in this paper:

$$\tilde{c}_{i+1/2}=\sqrt{\frac{g}{2}\left(\frac{A_i}{B_i}+\frac{A_{i+1}}{B_{i+1}}\right)}$$

The wavestrengths $\tilde{\alpha}_{1,2}$ can be computed from Equation (10):

$$\tilde{\alpha}_1=\frac{(\tilde{c}-\tilde{u})\Delta A+\Delta Q}{2\tilde{c}}$$
$$\tilde{\alpha}_2=\frac{(\tilde{c}+\tilde{u})\Delta A-\Delta Q}{2\tilde{c}}$$

Roe's solver, under certain circumstances, can lead to entropy violating solutions with spurious oscillation near a transcritical point. To rectify this problem, the 'entropy fix' proposed by Harten and Hyman [14] is used

$$|\tilde{\lambda}|=\begin{cases} |\tilde{\lambda}| & (|\tilde{\lambda}|\geqslant\varepsilon) \\ \varepsilon & (|\tilde{\lambda}|<\varepsilon) \end{cases}$$

where ε is given by

$$\varepsilon=\max(0,\tilde{\lambda}_{i+1/2}-\lambda_i,\lambda_{i+1}-\tilde{\lambda}_{i+1/2})$$

4.1.2. Homogeneous form of Roe's scheme. The integrated intercell numerical flux $\mathbf{H}^*_{i+1/2}$ can be easily obtained by modifying $\mathbf{F}^*_{i+1/2}$

$$\mathbf{H}^*_{i+1/2}=\tfrac{1}{2}(\mathbf{H}_{i+1}+\mathbf{H}_i)-\tfrac{1}{2}|\tilde{\mathbf{J}}|\Delta\mathbf{U}'_{i+1/2}$$

where the flux term $\mathbf{F}$ is replaced by $\mathbf{H}$ and $|\tilde{\mathbf{J}}|\Delta\mathbf{U}$ term related to the splitting of the flux difference $\Delta\mathbf{F}$ is replaced by $|\tilde{\mathbf{J}}|\Delta\mathbf{U}'$ corresponding to the splitting of $\Delta\mathbf{H}$. The definition of the term $\Delta\mathbf{U}'=(\Delta A',\Delta Q')^{\mathrm{T}}$ can be obtained by considering the relation

$$\Delta\mathbf{H}_{i+1/2}=\Delta\mathbf{F}_{i+1/2}-\Delta\mathbf{R}_{i+1/2}=\tilde{\mathbf{J}}_{i+1/2}\Delta\mathbf{U}'_{i+1/2} \tag{12}$$

DOI: 10.1002/fld

because the effect of the source flux $\mathbf{R}$ propagates along the eigenvalues $\tilde{\lambda}_{1,2}$ of Jacobian $\tilde{\mathbf{J}}$. The term $\Delta\mathbf{U}'$ represents the spatial difference of the conserved variables due to the source flux $\Delta\mathbf{R}$ as well as the momentum flux $\Delta\mathbf{F}$ while $\Delta\mathbf{U}$ is only related to $\Delta\mathbf{F}$. From Equation (12),

$$\begin{pmatrix} \Delta Q \\ \Delta\left(\dfrac{Q^2}{A}\right)+g\Delta I_1 \end{pmatrix}_{i+1/2} - \begin{pmatrix} 0 \\ g\Delta I_1 - g(\Omega_o+\Omega_f) \end{pmatrix}_{i+1/2} = \begin{pmatrix} 0 & 1 \\ -\tilde{\lambda}_1\cdot\tilde{\lambda}_2 & \tilde{\lambda}_1+\tilde{\lambda}_2 \end{pmatrix}_{i+1/2} \begin{pmatrix} \Delta A' \\ \Delta Q' \end{pmatrix}_{i+1/2}$$

and

$$\Delta Q'_{i+1/2} = \Delta Q_{i+1/2}$$

$$\Delta A'_{i+1/2} = -\frac{\Delta\left(Q^2/A\right)_{i+1/2} + g(\Omega_o+\Omega_f)_{i+1/2} - (\tilde{\lambda}_1+\tilde{\lambda}_2)\Delta Q_{i+1/2}}{\tilde{\lambda}_1\cdot\tilde{\lambda}_2}$$

Finally, the integrated flux $\mathbf{H}^*$ can be expressed as the following characteristic form:

$$\mathbf{H}^*_{i+1/2} = \frac{1}{2}(\mathbf{H}_{i+1}+\mathbf{H}_i) - \frac{1}{2}\sum_k (\tilde{\alpha}'_k|\tilde{\lambda}_k|\tilde{e}_k)_{i+1/2}$$

where the modified wave strengths $\tilde{\alpha}'_{1,2}$ are obtained from $\Delta\mathbf{U}' = \sum_k (\tilde{\alpha}'_k\tilde{e}_k)$ and given by

$$\tilde{\alpha}'_1 = \frac{(\tilde{c}-\tilde{u})\Delta A' + \Delta Q}{2\tilde{c}}$$

$$\tilde{\alpha}'_2 = \frac{(\tilde{c}+\tilde{u})\Delta A' - \Delta Q}{2\tilde{c}}$$

The wavestrengths $\tilde{\alpha}'_{1,2}$ represent the real state of the flow including the effect of the source terms. For example, in the case of the still water problem, $\Delta A' = 0$, $\Delta Q' = 0$ and, consequently, $\tilde{\alpha}'_{1,2} = 0$, which means that there is no flow through the cell interface.

4.2. HLL approximate Riemann solver

4.2.1. Original HLL scheme. The HLL solver was proposed by Harten *et al.* [1] and has been widely used because it has a simple structure and does not need complicated characteristic decomposition of the flux difference. The solution of the HLL solver consists of three constant states separated by two characteristics $\lambda_{\min}$ and $\lambda_{\max}$ as shown in Figure 2. The numerical flux in the intermediate region $\mathbf{F}(\mathbf{U}^*)$ can be obtained by considering the following two Rankine–Hugoniot conditions

$$\mathbf{F}(\mathbf{U}^*) - \mathbf{F}(\mathbf{U}_i) = \lambda_{\min}(\mathbf{U}^* - \mathbf{U}_i)$$

$$\mathbf{F}(\mathbf{U}_{i+1}) - \mathbf{F}(\mathbf{U}^*) = \lambda_{\max}(\mathbf{U}_{i+1} - \mathbf{U}^*)$$

and by eliminating the $\mathbf{U}^*$ term

$$\mathbf{F}(\mathbf{U}^*) = \frac{\lambda_{\max}\mathbf{F}(\mathbf{U}_i) - \lambda_{\min}\mathbf{F}(\mathbf{U}_{i+1})}{\lambda_{\max}-\lambda_{\min}} - \frac{\lambda_{\max}\lambda_{\min}(\mathbf{U}_{i+1}-\mathbf{U}_i)}{\lambda_{\max}-\lambda_{\min}}$$

DOI: 10.1002/fld

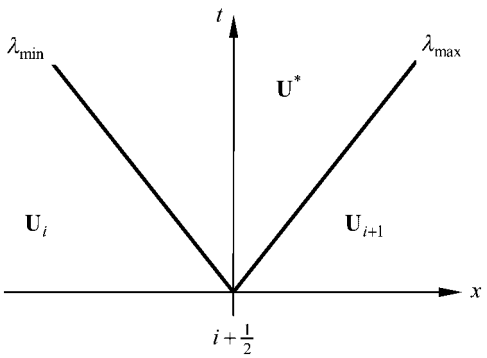

Figure 2. The solution structure of the HLL Riemann solver.

The intercell numerical flux $\mathbf{F}^*_{i+1/2}$ has different values according to the sign of the wave speeds and is given by

$$\mathbf{F}^*_{i+1/2} = \begin{cases} \mathbf{F}(\mathbf{U}_i) & \text{if } \lambda_{\min} \geqslant 0 \\ \mathbf{F}(\mathbf{U}_{i+1}) & \text{if } \lambda_{\max} \leqslant 0 \\ \mathbf{F}(\mathbf{U}^*) & \text{otherwise} \end{cases}$$

The two wave speeds $\lambda_{\min}$ and $\lambda_{\max}$ should be chosen carefully so as not to cause entropy violation and, in this paper, those suggested by Einfeldt [15] which use Roe's average values $\tilde{u}$ and $\tilde{c}$ are used

$$\lambda_{\min} = \min(u_i - c_i,\ \tilde{u}_{i+1/2} - \tilde{c}_{i+1/2})$$
$$\lambda_{\max} = \max(u_{i+1} + c_{i+1},\ \tilde{u}_{i+1/2} + \tilde{c}_{i+1/2})$$

where u and c represent velocity and wave speed, respectively.

4.2.2. Homogeneous form of HLL scheme. The integrated numerical flux $\mathbf{H}^*_{i+1/2}$ can be easily obtained by modifying the solution for the numerical flux $\mathbf{F}^*_{i+1/2}$

$$\mathbf{H}^*_{i+1/2} = \begin{cases} \mathbf{H}_i & \text{if } \lambda_{\min} \geqslant 0 \\ \mathbf{H}_{i+1} & \text{if } \lambda_{\max} \leqslant 0 \\ \mathbf{H}^* & \text{otherwise} \end{cases}$$

with

$$\mathbf{H}^* = \frac{\lambda_{\max}\mathbf{H}_i - \lambda_{\min}\mathbf{H}_{i+1}}{\lambda_{\max} - \lambda_{\min}} - \frac{\lambda_{\min}\lambda_{\max}\Delta\mathbf{U}'_{i+1/2}}{\lambda_{\max} - \lambda_{\min}}$$

where $\Delta\mathbf{U}' = (\Delta A', \Delta Q')^{\mathrm{T}}$ can be defined by using a technique similar to that used for Roe's solver. In other words, $\Delta\mathbf{U}'$ satisfy the following relation:

$$\Delta\mathbf{H}_{i+1/2} = \Delta\mathbf{F}_{i+1/2} - \Delta\mathbf{R}_{i+1/2} = \mathbf{J}^{\mathrm{hll}}_{i+1/2}\Delta\mathbf{U}'_{i+1/2} \tag{13}$$

DOI: 10.1002/fld

In this case, the new Jacobian matrix $\mathbf{J}^{\text{hll}}$ is used instead of Roe's approximate Jacobian $\tilde{\mathbf{J}}$ because the HLL solver has a different solution structure from Roe's solver. The Jacobian matrix for HLL solver, $\mathbf{J}^{\text{hll}}$, is considered as having two eigenvalues $\lambda_{\min}$ and $\lambda_{\max}$ and can be expressed as

$$\mathbf{J}^{\text{hll}}_{i+1/2} = \begin{pmatrix} 0 & 1 \\ -\lambda_{\min} \cdot \lambda_{\max} & \lambda_{\min} + \lambda_{\max} \end{pmatrix}_{i+1/2}$$

By solving Equation (13),

$$\Delta Q'_{i+1/2} = \Delta Q_{i+1/2}$$

$$\Delta A'_{i+1/2} = -\frac{\Delta\left(Q^2/A\right)_{i+1/2} + g(\Omega_o + \Omega_f)_{i+1/2} - (\lambda_{\min} + \lambda_{\max})\Delta Q_{i+1/2}}{\lambda_{\min} \cdot \lambda_{\max}}$$

4.3. TVD Lax–Wendroff scheme (TVD-LW)

4.3.1. Original TVD Lax–Wendroff scheme. The Lax–Wendroff scheme is second-order accurate and was initially presented by Lax and Wendroff [16]. The scheme can be derived based on the Taylor series expansion:

$$\mathbf{U}_i^{n+1} = \mathbf{U}_i^n + \left(\frac{\partial \mathbf{U}}{\partial t}\right)\Delta t + \left(\frac{\partial^2 \mathbf{U}}{\partial t^2}\right)\frac{(\Delta t)^2}{2} + \mathrm{O}(\Delta t)^3 \tag{14}$$

In case of a conservation law without source terms

$$\frac{\partial \mathbf{U}}{\partial t} = -\frac{\partial \mathbf{F}}{\partial x} \tag{15}$$

and

$$\frac{\partial^2 \mathbf{U}}{\partial t^2} = -\frac{\partial}{\partial t}\frac{\partial \mathbf{F}}{\partial x} = \frac{\partial}{\partial x}\left(-\mathbf{J}\frac{\partial \mathbf{U}}{\partial t}\right) = \frac{\partial}{\partial x}\left(\mathbf{J}\frac{\partial \mathbf{F}}{\partial x}\right) \tag{16}$$

By substituting (15) and (16) into (14)

$$\mathbf{U}_i^{n+1} = \mathbf{U}_i^n - \left(\frac{\partial \mathbf{F}}{\partial x}\right)\Delta t + \frac{\partial}{\partial x}\left(\mathbf{J}\frac{\partial \mathbf{F}}{\partial x}\right)\frac{(\Delta t)^2}{2} + \mathrm{O}(\Delta t)^3$$

Finally, by using a central difference approximation for the spatial derivatives and neglecting higher-order terms, the Lax–Wendroff scheme can be expressed as

$$\mathbf{U}_i^{n+1} = \mathbf{U}_i^n - \frac{1}{2}\frac{\Delta t}{\Delta x}(\mathbf{F}_{i+1} - \mathbf{F}_{i-1}) + \frac{1}{2}\left(\frac{\Delta t}{\Delta x}\right)^2 (\mathbf{J}_{i+1/2}[\mathbf{F}_{i+1} - \mathbf{F}_i] - \mathbf{J}_{i-1/2}[\mathbf{F}_i - \mathbf{F}_{i-1}])$$

This can be rewritten as a conservative form and given by

$$\mathbf{U}_i^{n+1} = \mathbf{U}_i^n - \frac{\Delta t}{\Delta x}(\mathbf{F}^*_{i+1/2} - \mathbf{F}^*_{i-1/2})$$

DOI: 10.1002/fld

with intercell numerical flux

$$\mathbf{F}^*_{i+1/2} = \frac{1}{2}(\mathbf{F}_i + \mathbf{F}_{i+1}) - \frac{1}{2}\frac{\Delta t}{\Delta x}(\mathbf{J}\Delta\mathbf{F})_{i+1/2} \tag{17}$$

Equation (17) can be rewritten as

$$\mathbf{F}^*_{i+1/2} = \frac{1}{2}(\mathbf{F}_i + \mathbf{F}_{i+1}) - \frac{1}{2}(|\mathbf{J}|\Delta\mathbf{U})_{i+1/2} + \frac{1}{2}\left(|\mathbf{J}|\left[1 - \frac{\Delta t}{\Delta x}|\mathbf{J}|\right]\Delta\mathbf{U}\right)_{i+1/2} \tag{18}$$

which can be considered as a first-order scheme with a second-order correction term. The main defect of using Lax–Wendroff scheme is that it produces spurious oscillations near discontinuous solutions. This problem can be solved by limiting the second-order correction term in Equation (18), which causes numerical oscillations near discontinuities. By using the characteristic decomposition technique used for Roe's scheme, the numerical flux function for TVD Lax–Wendroff scheme can be written as [7, 17]

$$\mathbf{F}^*_{i+1/2} = \frac{1}{2}(\mathbf{F}_i + \mathbf{F}_{i+1}) - \frac{1}{2}\sum_k (\tilde{\alpha}_k|\tilde{\lambda}_k|\tilde{e}_k)_{i+1/2} + \frac{1}{2}\sum_k \left(\tilde{\alpha}_k \Phi_k |\tilde{\lambda}_k|\left[1 - \frac{\Delta t}{\Delta x}|\tilde{\lambda}_k|\right]\tilde{e}_k\right)_{i+1/2}$$

where $\Phi_k = \Phi(r_k)$ is a nonlinear flux limiter function and the argument r_k represents the behaviour of the solution. The value of r_k is calculated from the ratio of wave strength $\tilde{\alpha}_k$ such as

$$r_k = \frac{\tilde{\alpha}_k^{\text{upwind}}}{\tilde{\alpha}_k^{\text{local}}}$$

4.3.2. Homogeneous form of TVD Lax–Wendroff scheme. The homogeneous form of Lax–Wendroff scheme can be constructed by replacing the flux term $\mathbf{F}$ with the integrated flux term $\mathbf{H}$. The modification is simpler than first-order schemes because it does not include the $\Delta\mathbf{U}$ term. The conservative form of Lax–Wendroff scheme can be rewritten as

$$\mathbf{U}_i^{n+1} = \mathbf{U}_i^n - \frac{\Delta t}{\Delta x}(\mathbf{H}^*_{i+1/2} - \mathbf{H}^*_{i-1/2})$$

with integrated intercell numerical flux

$$\mathbf{H}^*_{i+1/2} = \frac{1}{2}(\mathbf{H}_i + \mathbf{H}_{i+1}) - \frac{1}{2}\frac{\Delta t}{\Delta x}(\mathbf{J}\Delta\mathbf{H})_{i+1/2}$$

Similarly, the TVD version of the Lax–Wendroff numerical flux can be expressed as

$$\mathbf{H}^*_{i+1/2} = \frac{1}{2}(\mathbf{H}_i + \mathbf{H}_{i+1}) - \frac{1}{2}\sum_k (\tilde{\alpha}'_k|\tilde{\lambda}_k|\tilde{e}_k)_{i+1/2} + \frac{1}{2}\sum_k \left(\tilde{\alpha}'_k \Phi_k |\tilde{\lambda}_k|\left[1 - \frac{\Delta t}{\Delta x}|\tilde{\lambda}_k|\right]\tilde{e}_k\right)_{i+1/2}$$

where $\tilde{\alpha}'_k$ is the same modified wavestrength used for homogeneous form of Roe's scheme in Section 4.1. The flux limiter function $\Phi_k = \Phi(r_k)$ should also be modified to deliver the effect of the source terms into the TVD correction term and the argument r_k is calculated by using the ratio of modified wave strength $\tilde{\alpha}'_k$ like

$$r_k = \frac{\tilde{\alpha}_k'^{\text{upwind}}}{\tilde{\alpha}_k'^{\text{local}}}$$

DOI: 10.1002/fld

It is important to use $\tilde{\alpha}'_k$, instead of $\tilde{\alpha}_k$, to calculate the value of r_k because $\tilde{\alpha}'_k$ represents the real behaviour of the solutions including the effects of channel geometry and the using of $\tilde{\alpha}_k$ does not guarantee oscillation-free second-order solutions. A similar expression was mentioned by Burguete and Garcia-Navarro [8].

4.4. TVD MacCormack scheme (TVD-MC)

4.4.1. Original TVD MacCormack scheme. An alternative way to achieve second-order accuracy is using a two-step predictor–corrector technique. MacCormack [18] presented a second-order two-step method that does not require the computation of the Jacobian matrix and its eigenvalues. The scheme has been widely used [19–21] because of its efficiency and simple structure.

MacCormack scheme consists of two substeps: i.e. predictor and corrector steps, in which one-sided differencing is used in alternate directions:

Predictor step:

$$\mathbf{U}_i^p = \mathbf{U}_i^n - \frac{\Delta t}{\Delta x}(\mathbf{F}_{i+1}^n - \mathbf{F}_i^n)$$

Corrector step:

$$\mathbf{U}_i^c = \mathbf{U}_i^p - \frac{\Delta t}{\Delta x}(\mathbf{F}_i^p - \mathbf{F}_{i-1}^p)$$

Finally, the updated solution is given by

$$\mathbf{U}_i^{n+1} = \tfrac{1}{2}(\mathbf{U}_i^n + \mathbf{U}_i^c)$$

However, the problem with the MacCormack scheme is that it shows oscillatory behaviour near discontinuities like other classical second-order schemes. To rectify this problem, the TVD-MC scheme was presented by Garcia-Navarro *et al.* [22]. In the TVD version of MacCormack scheme, the TVD correction term is added to the final update step to eliminate oscillations

$$\mathbf{U}_i^{n+1} = \frac{1}{2}(\mathbf{U}_i^n + \mathbf{U}_i^c) + \frac{\Delta t}{\Delta x}(\mathbf{D}_{i+1/2}^n - \mathbf{D}_{i-1/2}^n)$$

where $\mathbf{D}^n$ is the TVD correction term. The form of the $\mathbf{D}$ term was obtained by using the similar technique used for TVD-LW scheme and expressed as

$$\mathbf{D}_{i+1/2}^n = \frac{1}{2}\sum_k \left(\tilde{\alpha}_k|\tilde{\lambda}_k|\left[1 - \frac{\Delta t}{\Delta x}|\tilde{\lambda}_k|\right][1-\Phi_k]\tilde{e}_k\right)_{i+1/2}$$

where the variables $\tilde{\alpha}_k$, $\tilde{\lambda}_k$ and $\tilde{e}_k$ are calculated by using Roe's method and Φ_k is a flux limiter function.

4.4.2. Homogeneous form of TVD-MC scheme. The homogeneous form of the MacCormack scheme can be easily obtained by replacing the flux term $\mathbf{F}$ with the integrated flux term $\mathbf{H}$ in each step:

Predictor step:

$$\mathbf{U}_i^p = \mathbf{U}_i^n - \frac{\Delta t}{\Delta x}(\mathbf{H}_{i+1}^n - \mathbf{H}_i^n)$$

DOI: 10.1002/fld

Corrector step:

$$\mathbf{U}_i^c = \mathbf{U}_i^p - \frac{\Delta t}{\Delta x}(\mathbf{H}_i^p - \mathbf{H}_{i-1}^p)$$

Then, the updated solution is given by

$$\mathbf{U}_i^{n+1} = \tfrac{1}{2}(\mathbf{U}_i^n + \mathbf{U}_i^c)$$

By using the integrated flux term $\mathbf{H}$, the contribution of the source terms is automatically evaluated in a different direction at each step and no special treatment is needed. In the case of the TVD-MC scheme, the TVD correction term should be modified to calculate the effect of the source terms correctly. This can be done by using the same expressions of $\tilde{\alpha}'$ and Φ_k used for TVD-LW scheme and the TVD correction term is expressed as

$$\mathbf{D}_{i+1/2}^n = \frac{1}{2}\sum_k \left(\tilde{\alpha}_k' |\tilde{\lambda}_k| \left[1 - \frac{\Delta t}{\Delta x} |\tilde{\lambda}_k| \right] [1 - \Phi_k] \tilde{e}_k \right)_{i+1/2}$$

5. NUMERICAL TESTS AND RESULTS

In this section, the proposed homogeneous form of conservative numerical schemes is applied to several benchmark tests that are taken from the available literature. All the test problems are simulated with a rectangular or trapezoidal channel as shown in Figure 3. The side slope of the trapezoidal channel is defined as $1:m$ and, in case of rectangular channel, m is set to zero. To ensure numerical stability CFL $= 0.9$ is used and the minmod flux limiter function that is given by $\Phi(r) = \max[0, \min(1, r)]$ is used for TVD schemes. The convergence criterion for steady problems is defined as $R < 1 \times 10^{-6}$, where R is the relative error defined by

$$R = \sqrt{\sum_i \left(\frac{h_i^n - h_i^{n-1}}{h_i^n} \right)^2}$$

The boundary conditions are described by using a ghost-cell approach in which the conditions are implemented by creating dummy cells at the end of the reach. For example, the values for the summy cells to describe transmissive downstream boundary are defined as

$$A_{N+1} = A_N, \quad Q_{N+1} = Q_N$$

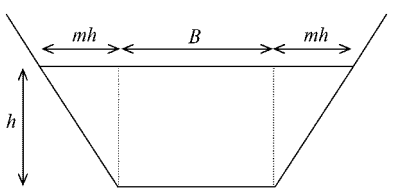

Figure 3. Cross section used for test problems.

DOI: 10.1002/fld

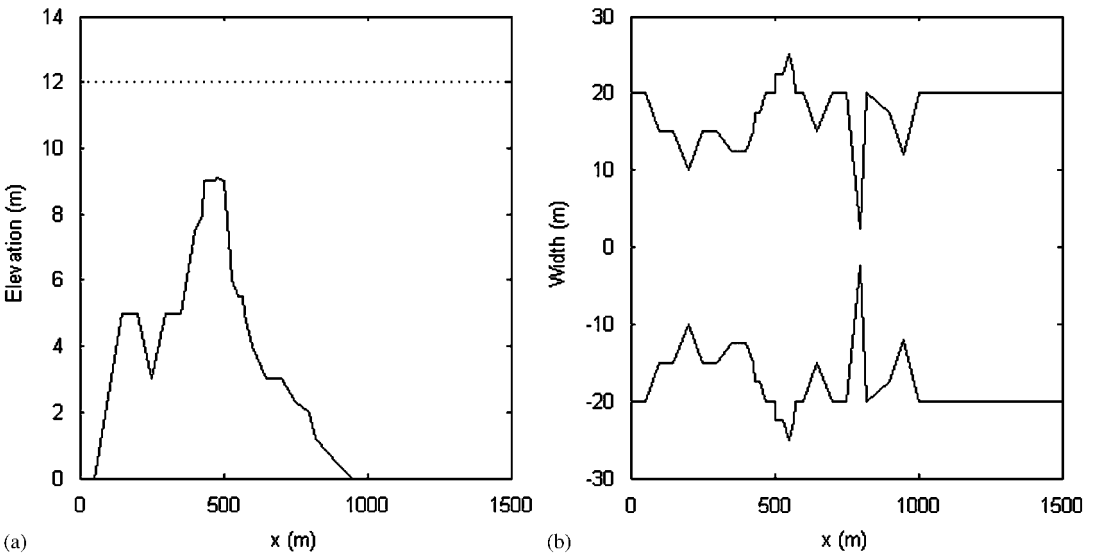

Figure 4. Bed elevation and width variation for Problems 1 and 2.

and

$$A_{N+2} = A_{N-1}, \quad Q_{N+2} = Q_{N-1}$$

Problem 1 (*Quiescent flow*)
This problem is chosen to illustrate the benefit of the homogeneous form of the equations, which can achieve perfect balance of two flux terms **F** and **R**. Many numerical schemes fail to maintain quiescent flow without special treatment of the source terms. This problem was presented by Goutal and Maurel [23] and consists of stationary flow with uniform water surface level $z_s = 12\,\text{m}$ and a channel with variable bed slope and width. The channel geometry for this problem is depicted in Figure 4. The length of the channel is 1500 m and 600 uniform cells ($\Delta x = 2.5\,\text{m}$) are used.

Numerical solutions are presented in Figure 5. To show the benefit of using homogeneous form schemes, the numerical results at $t = 10\,000\,\text{s}$ are compared with the solutions calculated by the original schemes with pointwise source term treatment as well as the exact solutions. As shown in the figure, all the proposed schemes reproduce quiescent flow correctly without any numerical errors, while the pointwise method fails to maintain a stationary state. In this case, the integrated numerical flux $\mathbf{H}^*$ is zero at each cell interface because the modified variable differences $\Delta A' = \Delta Q' = 0$ throughout the whole domain. This shows that there is no transfer of mass and momentum through each cell interface and, consequently, the homogeneous form of numerical schemes can ensure a stationary state.

Problem 2 (*Tidal wave flow over an irregular bed*)
To verify the ability to solve flow over an irregular bed, the proposed schemes are applied to a test case initially presented by Goutal and Maurel [23]. The same geometry (bed level and base

DOI: 10.1002/fld

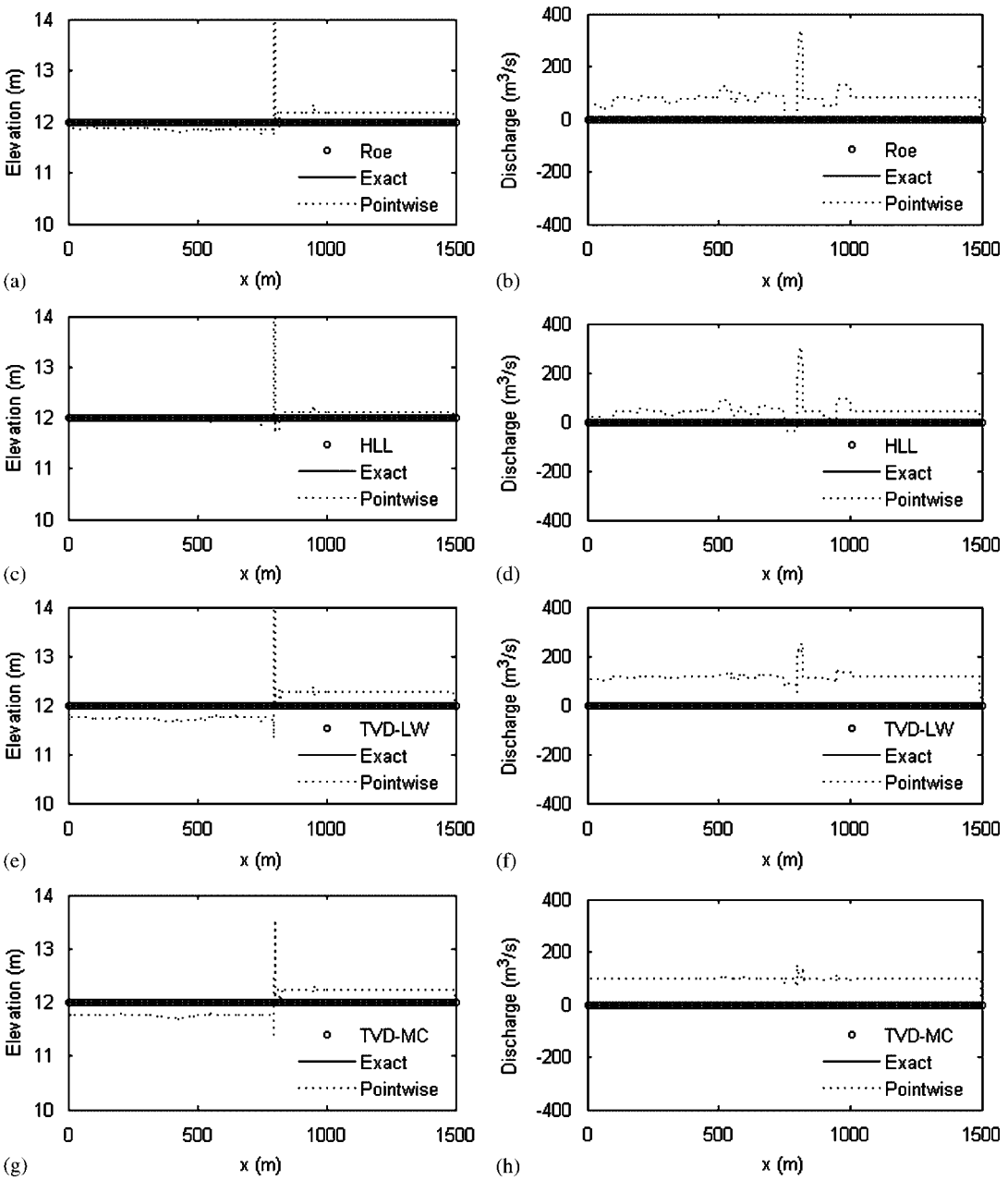

Figure 5. Water surface and discharge profiles in Problem 1: (a), (b) Roe; (c), (d) HLL; (e), (f) TVD-LW; and (g), (h) TVD-MC.

DOI: 10.1002/fld

width) as in Problem 1 is used. The initial conditions are the same as the previous problem

$$Q(x,0)=0\,\mathrm{m}^3/\mathrm{s}$$

$$h(x,0)+z_b=12\,\mathrm{m}$$

and the boundary conditions are

$$h(0,t)=h(0,0)+\phi(t)$$

$$Q(L,t)=0\,\mathrm{m}^3/\mathrm{s}$$

where $\phi(t)$ is the time-dependent tidal flow entering the boundary $x=0$ and given by

$$\phi(t)=4+4\sin\left(\pi\left(\frac{4t}{86\,400}+\frac{1}{2}\right)\right)$$

which represents a slow wave with long period $T=43\,200\,\mathrm{s}$. The friction term is included by setting Manning's roughness coefficient $n=0.1$. The analytical solutions were presented by Bermudez and Vazquez [5] and are obtained by the first-order approximation of the mass conservation equation:

$$h(x,t)=h(x,0)+\phi(t)$$

$$Q(x,t)=\phi'(t)\int_x^L (B(s)+2\,\mathrm{m\,h})\,\mathrm{d}s$$

The numerical simulations were performed with both a rectangular ($m=0$) and a trapezoidal channel ($m=1$) using 200 uniform cells with $\Delta x=7.5\,\mathrm{m}$. It should be noted that the analytical solutions are only asymptotically exact as the speed of flow tends to zero.

Numerical solutions are shown in Figures 6 and 7. The velocity profiles at $t=10\,800\,\mathrm{s}$ corresponding to a half-risen tide with maximum positive velocity are compared with exact solutions. As shown in the figures, all the proposed schemes calculate the effect of the extreme irregularity of the channel geometry correctly and show good agreement with the analytical solutions for both rectangular and trapezoidal channels. Especially, the TVD second-order schemes do not show numerical errors due to the imbalance of high-order numerical flux and source terms. This is because the high-order correction terms using the modified wave strength $\tilde{\alpha}'$ can deliver the effect of geometry and friction force to the high-order term and also because the numerical schemes automatically calculate the high-order source flux that is well balanced with the flux term $\mathbf{F}$.

Problem 3 (*Steady flow over an irregular bed with friction*)
MacDonald [24] presented an analytical solutions for steady open channel flow problems including a friction force term by calculating the bed slope S_o corresponding to a hypothetical water depth $\hat{h}$. In [24], the bed slope function $S_o(x)$ was obtained from the steady flow equation and given by

$$S_o(x)=\left(1-\frac{Q^2T}{gA^3}\right)\hat{h}'(x)+\frac{Q^2n^2P^{4/3}}{A^{10/3}}$$

DOI: 10.1002/fld

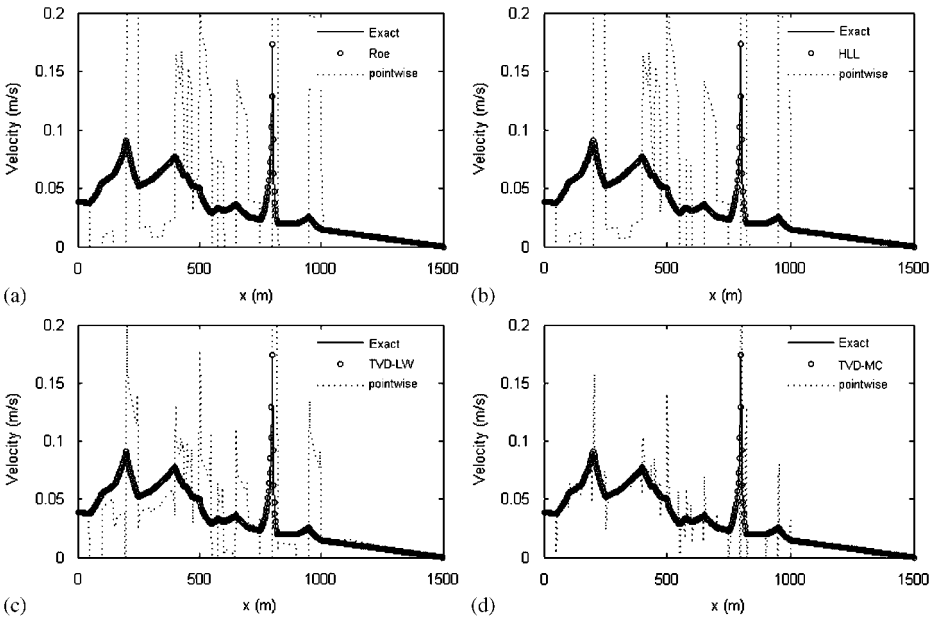

Figure 6. Velocity profiles in Problem 2 with a rectangular channel: (a) Roe; (b) HLL; (c) TVD-LW; and (d) TVD-MC.

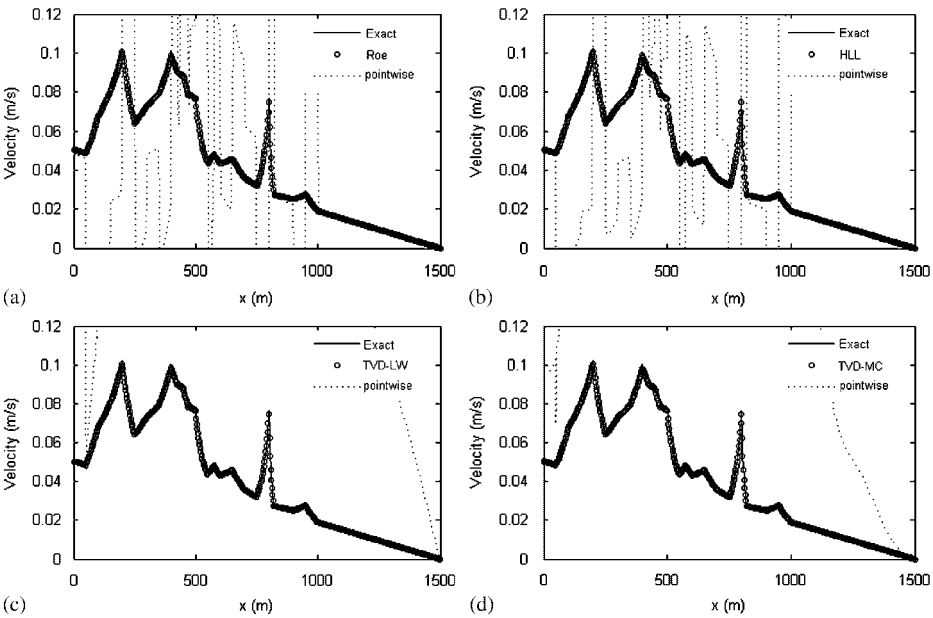

Figure 7. Velocity profiles in Problem 2 with a trapezoidal channel: (a) Roe; (b) HLL; (c) TVD-LW; and (d) TVD-MC.

DOI: 10.1002/fld

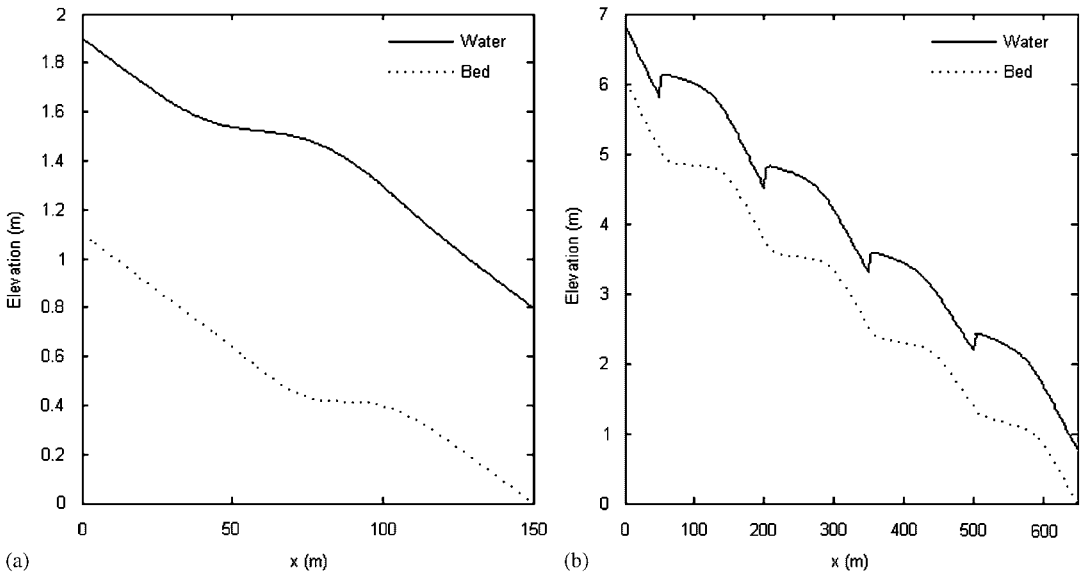

Figure 8. Water surface and bed elevation for Problem 3–1 and Problem 3–2.

where $T = B + 2m\hat{h}(x)$ is the top width of the wetted cross section, $P = B + 2\hat{h}(x)\sqrt{1+m^2}$ is the wetted perimeter and Q represents constant discharge. A set of test cases that consist of steady flows over rectangular or trapezoidal rough channel were presented in [24] and, among them, two problems with prismatic channels were chosen to verify the ability of the proposed numerical schemes. In Problems 3–1, a subcritical and smooth water depth profile is used in a rectangular channel, while a transcritical flow consisting of four hydraulic jumps is simulated in Problems 3–2. The bed and free surface profiles for both problems are depicted in Figure 8.

The numerical solutions are presented in Figures 9 and 10. The numerical water depth and discharge profiles are compared with the hypothetical depth $\hat{h}$ and steady discharge Q. As shown in Figure 9, all the proposed schemes produce very accurate solutions to this subcritical flow problem. The numerical solutions to Problems 3–2 are presented in Figure 10. This problem is a very severe test case including multiple hydraulic jumps and transcritical points. All the proposed schemes predicted the position and magnitude of the hydraulic jumps, except small discrepancies at the discharge profiles at the shock positions(which is a common numerical behaviour for most conservative schemes). The convergence histories for both cases are shown in Figure 11 and it shows that the TVD-MC scheme that is two-step predictor–corrector method converges to steady state faster than the other schemes. Generally, the two-step approach shows faster convergence than normal methods, while the former has a more complicated structure. It is clear that there is a tradeoff between accuracy and complexity.

Problem 4 (*Steady flow over a hump in a non-prismatic channel*)
A steady flow in a 3 m-long rectangular non-prismatic channel with a hump is simulated with the proposed schemes. This test case was presented by Hubbard and Garcia-Navarro [7] and the

DOI: 10.1002/fld

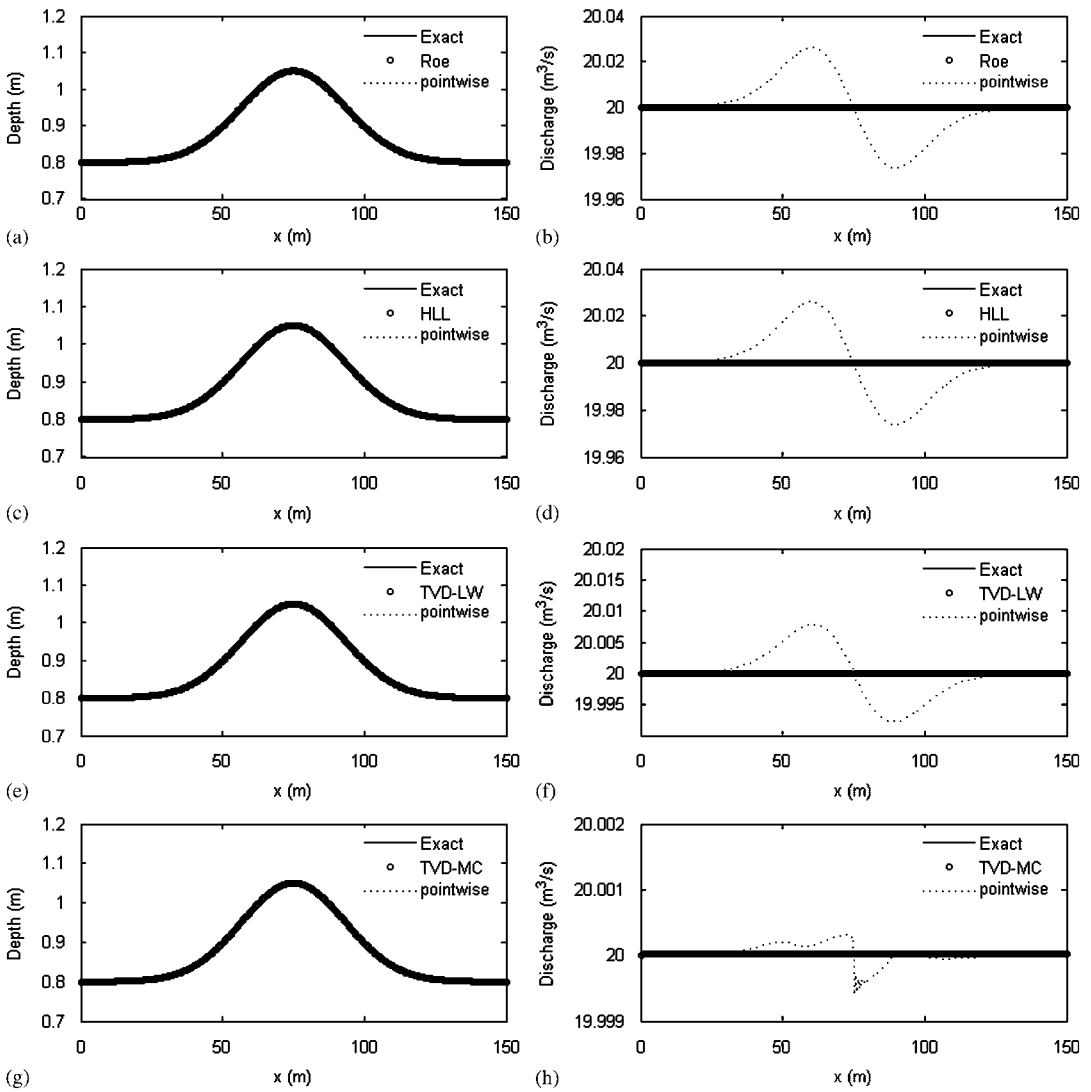

Figure 9. Water depth and discharge profiles in Problem 3–1: (a), (b) Roe; (c), (d) HLL; (e), (f) TVD-LW; and (g), (h) TVD-MC.

channel geometry is given by

$$z_b(x) = \begin{cases} 0.1\cos^2(\pi(x-1.5)), & 1.0 \leqslant x \leqslant 2.0 \\ 0.0 & \text{otherwise} \end{cases}$$

$$b(x) = \begin{cases} 1.0 - 0.1\cos^2(\pi(x-1.5)), & 1.0 \leqslant x \leqslant 2.0 \\ 1.0 & \text{otherwise} \end{cases}$$

DOI: 10.1002/fld

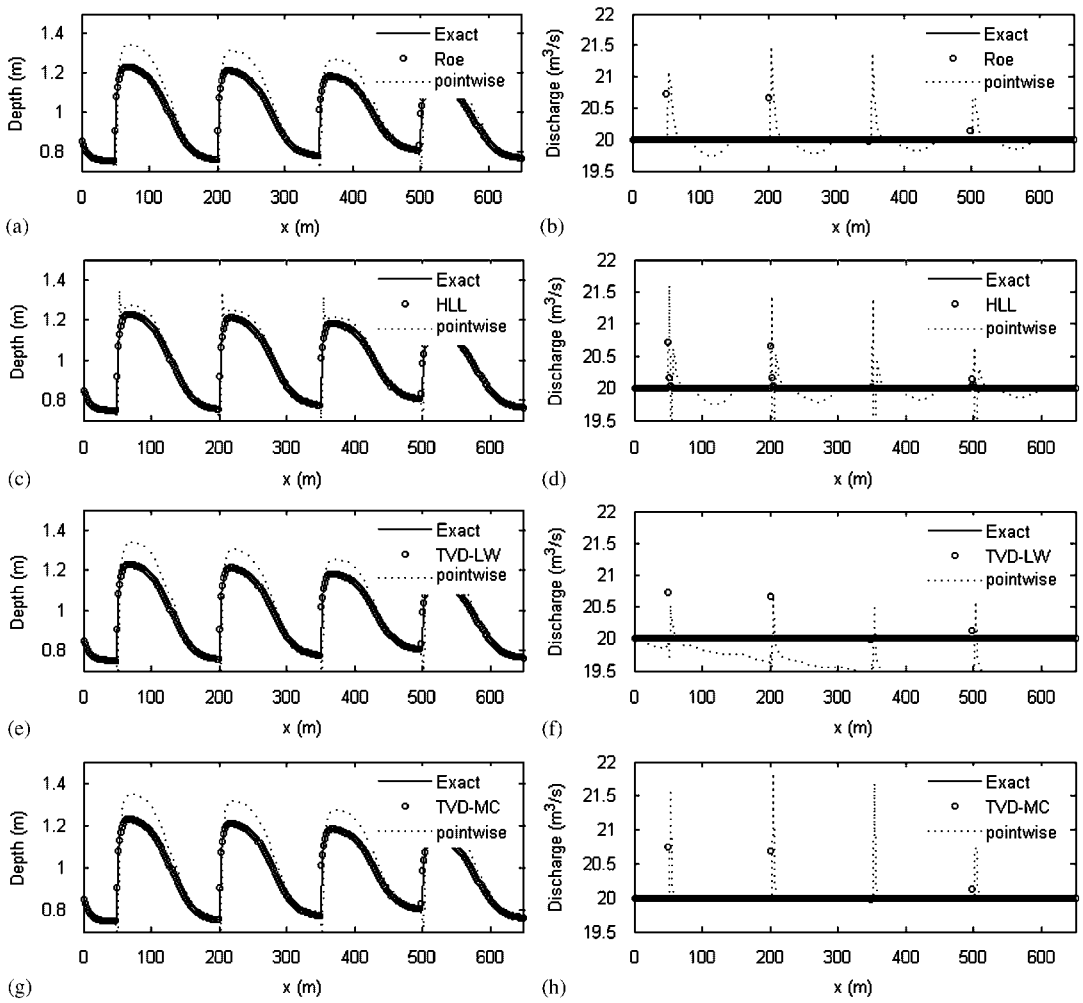

Figure 10. Water depth and discharge profiles in Problem 3–2: (a), (b) Roe; (c), (d) HLL; (e), (f) TVD-LW; and (g), (h) TVD-MC.

and shown in Figure 12. A uniform 150 cell grid with $\Delta x = 0.02\,\mathrm{m}$ is used for the two flows, each defined by a local Froude No. Fr: subcritical ($Fr = 0.5$) flow and transcritical ($Fr = 0.6$) flow. The downstream boundary condition is $h_{\mathrm{dn}} = 1\,\mathrm{m}$.

Numerical solutions are presented in Figures 13 and 14. Similar to the results of previous problems, all the proposed schemes predicted the water depth and discharge profiles correctly in the subcritical flow case. In case of transcritical flow problem, the proposed schemes reproduce the position and strength of the hydraulic jump very correctly. The convergence histories for this problems are shown in Figure 15. Similar to Problems 3–1 and 3–2, the TVD-MC scheme converges to steady state faster than other schemes.

DOI: 10.1002/fld

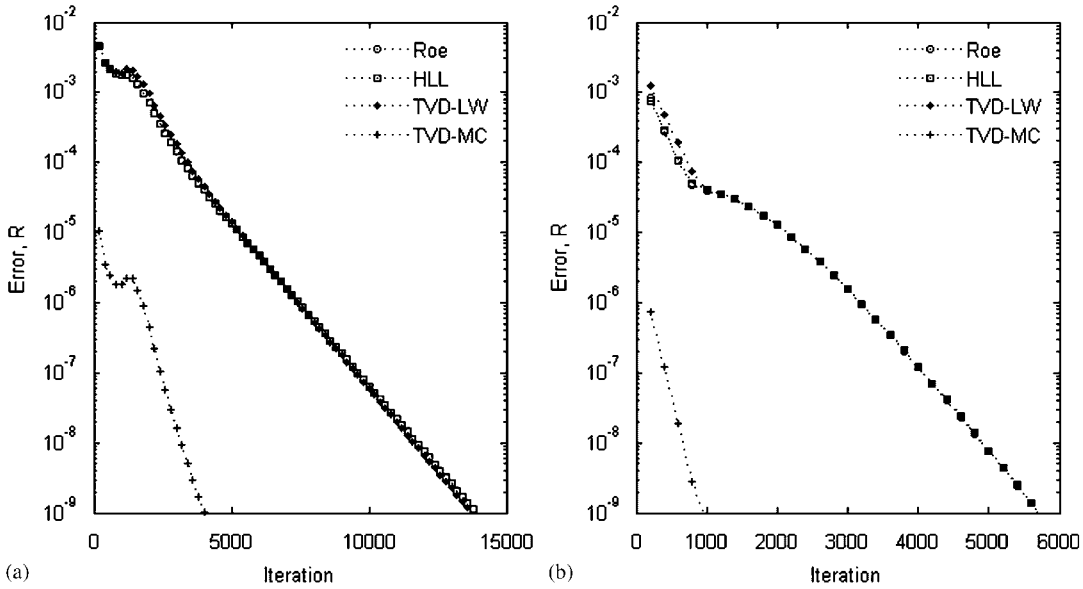

Figure 11. Convergence histories in: (a) Problem 3–1 and (b) Problem 3–2.

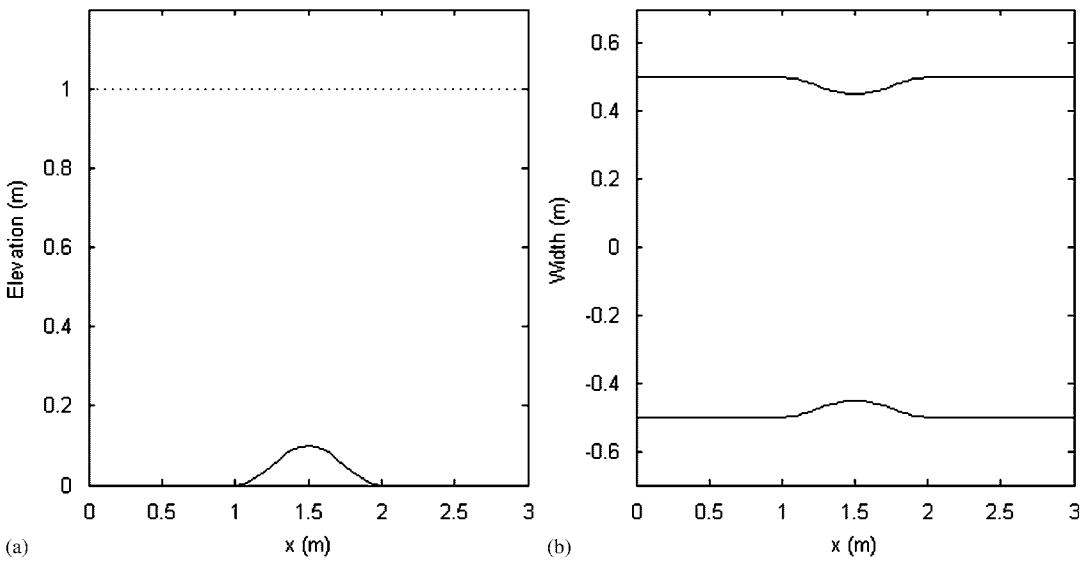

Figure 12. Bed elevation and width variation for Problem 4.

Problem 5 (*Wave propagation*)

The test problem presented by LeVeque [4] is chosen to demonstrate the ability of the proposed schemes to solve wave propagation problems over variable geometry. A 1 m-long rectangular

DOI: 10.1002/fld

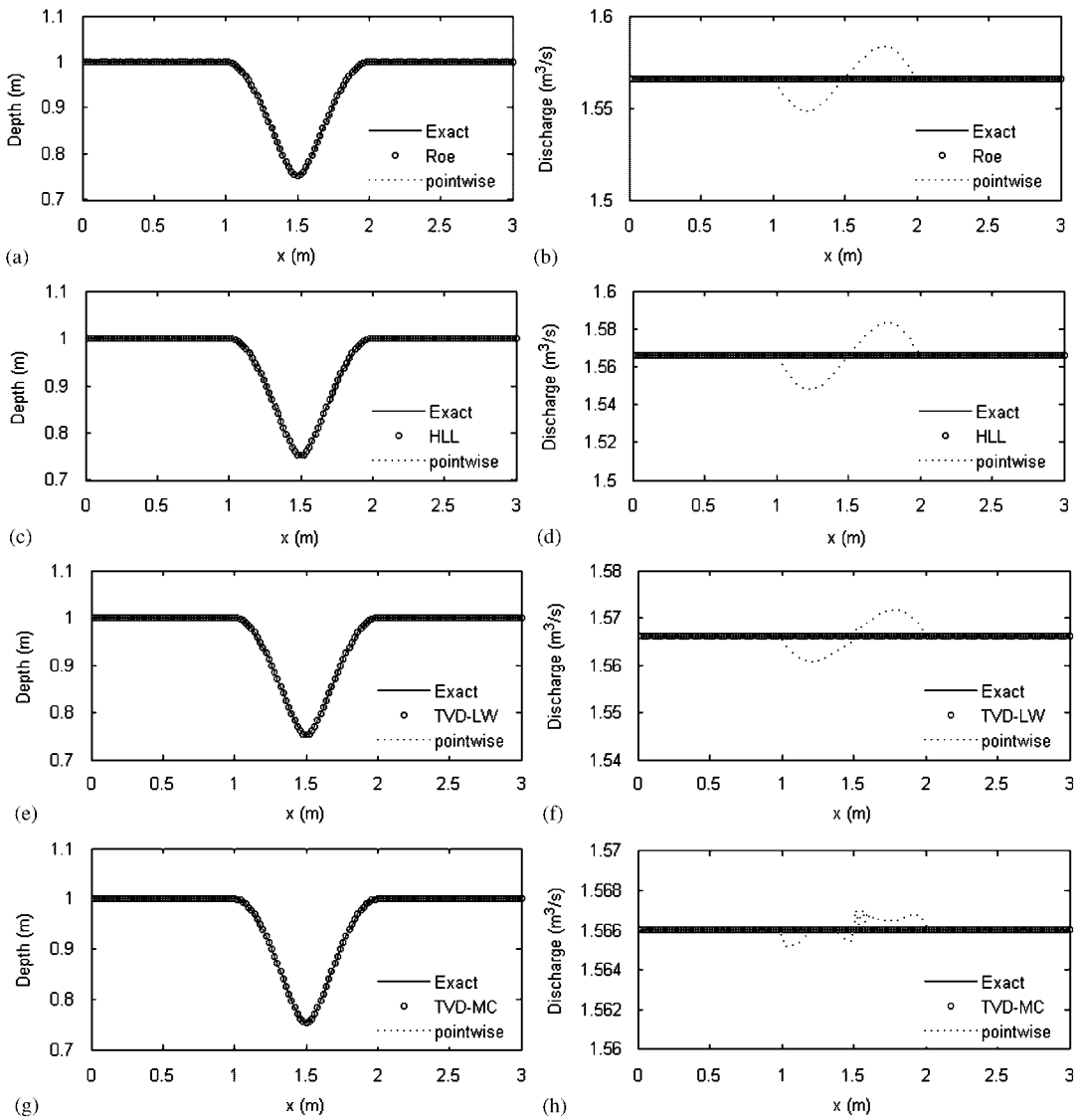

Figure 13. Water depth and discharge profiles in Problem 4 (subcritical case): (a), (b) Roe; (c), (d) HLL; (e), (f) TVD-LW; and (g), (h) TVD-MC.

channel with variable bed elevation, which is given by

$$z_b(x) = \begin{cases} 0.25\cos(\pi(x-0.5)/0.1+1.0), & 0.4 \leqslant x \leqslant 0.6 \\ 0.0 & \text{otherwise} \end{cases}$$

DOI: 10.1002/fld

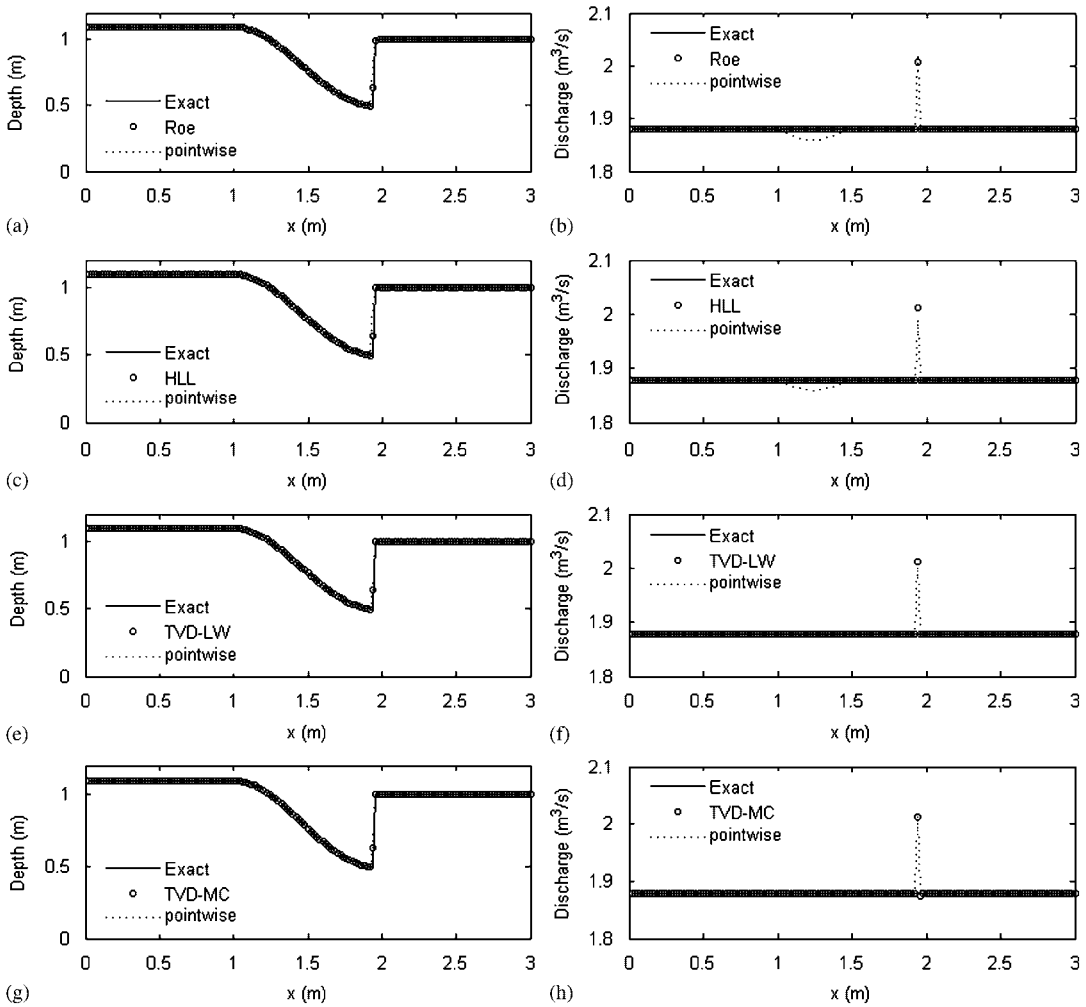

Figure 14. Water depth and discharge profiles in Problem 4 (transcritical case): (a), (b) Roe; (c), (d) HLL; (e), (f) TVD-LW; and (g), (h) TVD-MC.

is used and the initial condition is stationary flow ($Q=0$) with the following water surface profile:

$$z_s(x)=\begin{cases}1.0+\varepsilon, & 0.1\leqslant x\leqslant 0.2\\ 1.0 & \text{otherwise}\end{cases}$$

where ε is a small perturbation. According to [4], the reduced gravitational acceleration $g=1\,\mathrm{m}^2/\mathrm{s}$ and perturbation depth $\varepsilon=0.01$ are used. The initial perturbation of water depth causes two waves, right- and left-going, which propagates at the speed $\pm\sqrt{gh}$, respectively. The right-going wave propagates over the hump located at the middle area of the channel, whereas the left-going wave

DOI: 10.1002/fld

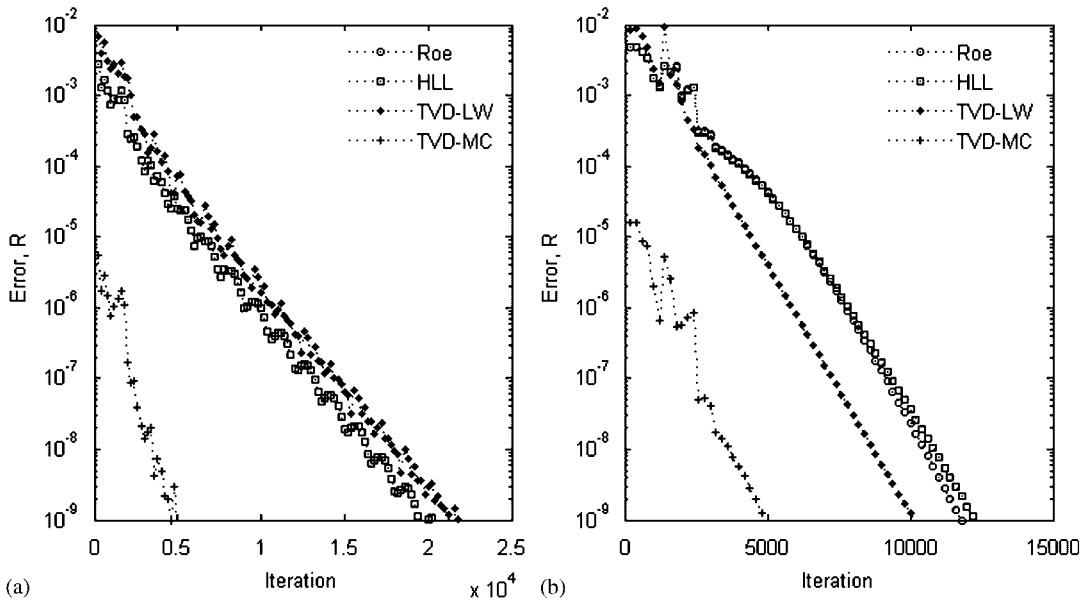

Figure 15. Convergence histories in Problem 4: (a) subcritical and (b) transcritical case.

leaves the domain through the boundary $x=0$. The numerical results are obtained at $t=0.7$ s on a uniform grid with 500 cells.

The numerical solutions are presented in Figure 16. Owing to the absence of analytical solutions, the computed solutions are compared with the reference solution obtained with TVD-LW scheme on a finer grid (2500 cell). As shown in the figure, the proposed schemes reproduce wave propagation of very small pertubation without any noticeable distortions or oscillations and the two TVD second-order schemes show more accurate solutions than the two first-order schemes.

In this case, a series of runs has been carried out to indicate the accuracy of the presented schemes. The l_2 errors are plotted against the corresponding cell numbers and shown in Figure 17. According to the numerical results, the second-order accurate schemes produce more accurate solutions and show higher sensitivity to the variation of the grid size.

6. CONCLUSIONS AND FUTURE POSSIBILITIES

A simple and accurate method to solve open channel flow over irregular geometry has been presented. The modification of the shallow water equations to the homogeneous form enables one to use numerical methods developed for homogeneous conservations laws and avoid a cumbersome fractional step method for source term treatment. An integrated numerical flux, which includes the representation of the source terms, has been obtained by straightforward modification of the governing equations. The well-known conservative numerical schemes have then been amended

DOI: 10.1002/fld

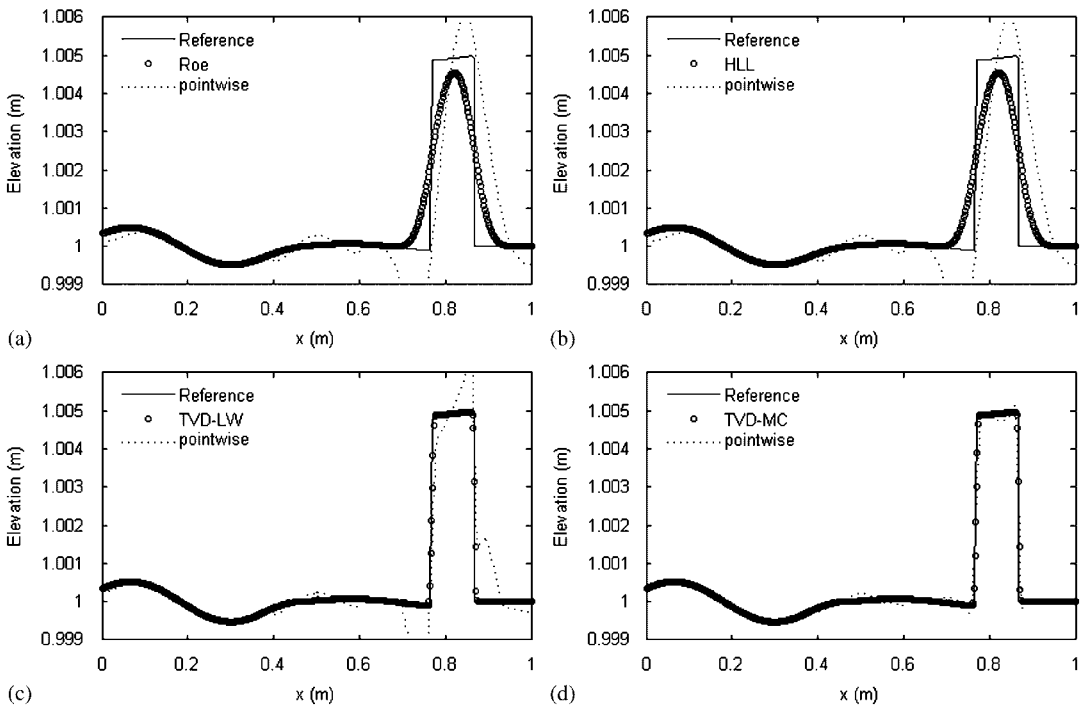

Figure 16. Water surface profiles in Problem 5: (a) Roe; (b) HLL; (c) TVD-LW; and (d) TVD-MC.

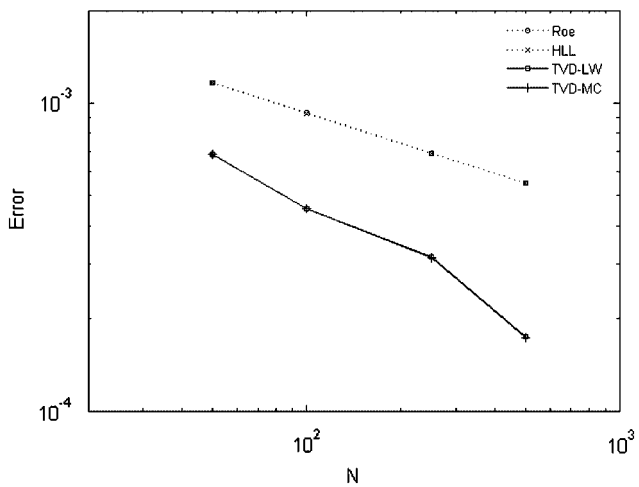

Figure 17. Graph of l_2 error against number of cells (N) in Problem 5.

to solve these newly proposed equations. The numerical results show that the proposed schemes are highly conservative and accurate while having simple forms. The proposed schemes produce excellent agreement with the analytical solutions.

DOI: 10.1002/fld

The proposed method has several advantages. First, it can solve steady flows over highly non-prismatic channels without numerical errors, thus demonstrating that the proposed schemes achieve perfect numerical balance of the two flux terms **F** and **R**. Second, it can compute the numerical flux corresponding to the real state of water flow and give straightforward results. For example, in the still water simulation problem, the integrated numerical flux $\mathbf{H}^*$ is equal to zero at every cell interface, which represents no transfer of mass and momentum. Third, high-order accuracy can be obtained easily and no special treatment is needed to maintain a numerical balance, because it is performed automatically in the integrated numerical flux function. Finally, the proposed approach has strong applicability to various conservative numerical schemes as shown in the numerical results.

The authors believe that it is straightforward to extend this methodology to real river flow and the two-dimensional equations. Preliminary results suggest that it may well assist with the wetting/drying boundary problem. Implementations and demonstrations of these will be published elsewhere.

ACKNOWLEDGEMENTS

S. Lee is grateful to the Korean Government for their financial support of his PhD studies.

REFERENCES

1. Harten A, Lax P, van Leer B. On upstream differencing and Godunov-type schemes for hyperbolic conservation laws. *SIAM Review* 1983; **25**(1):35–61.
2. Roe P. Approximate Riemann solvers, parameter vectors, and difference schemes. *Journal of Computational Physics* 1997; **135**:250–258.
3. Nujic M. Efficient implementation of non-oscillatory schemes for the computation of free-surface flows. *Journal of Hydraulic Research* 1995; **33**:101–111.
4. LeVeque R. Balancing source terms and flux gradients in high-resolution Godunov methods: the quasi-steady wave-propagation algorithm. *Journal of Computational Physics* 1998; **146**:346–365.
5. Bermudez A, Vazquez ME. Upwind methods for hyperbolic conservation laws with source terms. *Computers and Fluids* 1994; **23**:1049–1071.
6. Garcia-Navarro P, Vazquez-Cendon M. On numerical treatment of the source terms in the shallow water equations. *Computers and Fluids* 2000; **29**:951–979.
7. Hubbard M, Garcia-Navarro P. Flux difference splitting and the balancing of source terms and flux gradients. *Journal of Computational Physics* 2000; **165**:89–125.
8. Burguete J, Garcia-Navarro P. Efficient construction of high-resolution TVD conservative schemes for equations with source terms: application to shallow water flows. *International Journal for Numerical Methods in Fluids* 2001; **37**:209–248.
9. Burguete J, Garcia-Navarro P. Improving simple explicit methods for unsteady open channel and river flow. *International Journal for Numerical Methods in Fluids* 2004; **45**:125–156.
10. Zhou J, Causon D, Mingham C, Ingram D. The surface gradient method for the treatment of source terms in the shallow water equations. *Journal of Computational Physics* 2001; **168**:1–25.
11. Capart H, Eldho T, Huang S, Young D, Zech Y. Treatment of natural geometry in finite volume river flow computations. *Journal of Hydraulic Engineering* 2003; **129**(5):385–393.
12. Gascon LI, Corberan JM. Construction of second-order TVD schemes for nonhomogeneous hyperbolic conservation laws. *Journal of Computational Physics* 2001; **172**:261–297.
13. Cunge J, Holly F, Verwey A. *Practical Aspects of Computational River Hydraulics*. Pitman Publishing Limited: London, 1980.
14. Harten A, Hyman J. Self adjusting grid methods for one-dimensional hyperbolic conservation law. *Journal of Computational Physics* 1983; **50**:235–269.
15. Einfeldt B. On Godunov-type methods for gas dynamics. *SIAM Journal on Numerical Analysis* 1988; **25**:294–318.

DOI: 10.1002/fld

16. Lax PD, Wendroff B. Systems of conservation laws. *Communications on Pure and Applied Mathematics* 1960; **13**:217–237.
17. Jha AK, Akiyama J, Ura M. High resolution flux-difference-splitting scheme on adaptive grid for open-channel flows. *International Journal for Numerical Methods in Fluids* 2001; **36**:35–52.
18. MacCormack RW. Numerical solution of the interaction of a shock wave with a laminar boundary layer. *Proceedings of the 2nd International Conference on Numerical Methods in Fluid Dynamics*, Springer: Berlin, Germany, 1971; 151–163.
19. Garcia-Navarro P, Fras A, Villanueva I. Dam break simulation: some results for one-dimensional models of real cases. *Journal of Hydrology* 1999; **216**:227–247.
20. Garcia-Navarro P, Kahawitta RA. Numerical solution of the St. Venant equations with the Mac-Cormack finite difference scheme. *International Journal for Numerical Methods in Fluids* 1986; **6**:259–274.
21. Garcia-Navarro P, Saviron JM. McCormack's method for the numerical simulation of one-dimensional discontinuous unsteady open channel flow. *Journal of Hydraulic Research* 1992; **30**:95–105.
22. Garcia-Navarro P, Alcrudo F, Saviron JM. 1-D open channel flow simulation using TVD-McCormack scheme. *Journal of Hydraulic Engineering* 1992; **118**:1359–1372.
23. Goutal N, Maurel F. *Technical Report HE-43/97/016/A*, *Proceedings of the 2nd Workshop on Dam-break Wave Simulation*, Electricite de France, Department Laboratoire National d'Hydraulique, Groupe Hydraulique Fluviale, 1997.
24. Macdonald I. Analysis and computation of steady open channel flow. *Ph.D. Thesis*, University of Reading, 1996.

DOI: 10.1002/fld